Journal of Materials Chemistry A

PAPER

View Article Online
View Journal | View Issue

Cite this: J. Mater. Chem. A, 2014, 2, 339

Core–shell structured MgAl-LDO@Al-MS hexagonal nanocomposite: an all inorganic acid–base bifunctional nanoreactor for one-pot cascade reactions†

Ping Li,[ab] Yu Yu,[ab] Pei-Pei Huang,[ab] Hua Liu,[ab] Chang-Yan Cao[a] and Wei-Guo Song*[a]

Received 28th August 2013
Accepted 17th October 2013

DOI: 10.1039/c3ta13403b

www.rsc.org/MaterialsA

A core–shell structured nanocomposite, with hexagonal Mg–Al mixed oxide nanoplates derived from LDHs as the inner core and Al-containing mesoporous silica as the outer shell, was prepared using an inorganic, low cost and simple route. The mesoporous silica shell was not only capable of protecting the MgAl-LDO core, but also offered a high surface area for the derivation of functional acid catalytic sites. The MgAl-LDO@Al-MS nanocomposite served as an efficient acid–base bifunctional nanoreactor for one-pot multistep cascade reaction sequences, due to the good spatial separation of antagonistic sites *via* the core–shell structure design, confinement and enrichment effect of the reaction species endowed by the nanoreactor features.

1. Introduction

One-pot cascade reactions, which involve two or more steps in a single reaction vessel, are a sustainable and green way to synthesize structurally complex organic substances, as they can reduce the synthesis steps such as intermediate isolation and purification, save energy consumption, lower the operation cost, and decrease the amount of waste.[1–3] To make one-pot cascade reactions perform efficiently, multifunctional catalysts with two or more different functionalities coexisting compatibly within the same catalyst particles are required. A variety of multifunctional catalysts have been reported, and among them the acid–base bifunctional heterogeneous catalyst is one of the most important classes,[4–9] which is also the focus of this study.

To avoid the mutual neutralization of acid sites and base sites, precise control over the distribution of acidic and basic active sites to obtain spatial separation is generally a prerequisite.[10–12] To date, almost all the acid–base bifunctional heterogeneous catalysts reported are organic–inorganic silica-based composite materials.[13–18] These were successful catalysts, and some of them were produced by clever designs.[15–18] Yet these catalysts are produced by complicated routes, including grafting of organic groups, protecting acid or base precursors, and generating acid or base catalysts. Thus it is appealing to find a straightforward and low cost method to produce an acid–base bifunctional catalyst. In this study, we produced core–shell structured MgAl-LDO@Al-MS nanoplates by an inorganic-based, low cost and simple route.

Layered double hydroxides (LDHs) are a typical class of 2D nanostructured anionic clays, and consist of positively charged brucite-type layers and exchangeable anions situated in the interlayer space.[19] LDHs have cation-exchange ability of the brucite layer, anion-exchange ability of the interlayer, surface adsorption capacity, memory effect and surface tunable basicity, and have been widely used in catalysis, adsorption, water treatment, energy storage, functional composites, host–guest chemistry and drug delivery.[20–27] In particular, layered double oxides (LDOs) resulting from the calcination of LDHs are typical heterogeneous Lewis bases, and are able to act as efficient solid base catalysts for a broad spectrum of organic reactions, such as the epoxidation of olefins, *N*-oxidation of pyridines, and carbon–carbon bond-forming reactions.[28–32]

In this study, we chose LDH as the base source as well as a hard template for an acidic mesoporous silica coating, and produced core–shell structured MgAl-LDO@Al-MS hexagonal nanoplates. This was an inorganic acid–base bifunctional heterogeneous nanocatalyst system, with hexagonal Mg–Al mixed oxides nanoplates derived from LDHs as the inner core and Al-containing mesoporous silica as the outer shell. The synthesis method was straightforward. Due to the successful coexistence and site isolation of acid–base active sites, and the confinement reaction medium provided by the mesoporous structure, this integrated nanocomposite system with MgAl-LDO as basic sites and Al-MS as acid sites served as an excellent nanoreactor for catalyzing one-pot deprotection–Knoevenagel cascade reaction sequences.

[a]Beijing National Laboratory for Molecular Sciences (BNLMS), CAS Key Laboratory of Molecular Nanostructures and Nanotechnology, Institute of Chemistry, Chinese Academy of Sciences, Beijing, 100190, P. R. China. E-mail: wsong@iccas.ac.cn; Fax: +86-10-62557908

[b]Graduate University of Chinese Academy of Sciences, Beijing, 100049, P. R. China

† Electronic supplementary information (ESI) available: Characterization of the catalysts. See DOI: 10.1039/c3ta13403b

2. Experimental section

2.1. Materials and reagents

$MgCl_2 \cdot 6H_2O$, $AlCl_3 \cdot 6H_2O$, $Al(NO_3)_3 \cdot 9H_2O$, NaOH, Na_2CO_3 and ammonia solution (concentration 25 wt%) were purchased from Beijing Chemical Reagent Corporation (Beijing, China). Benzaldehyde dimethyl acetal, 4-methoxybenzaldehyde dimethyl acetal, methyl cyanoacetate and cetyltrimethylammonium bromide (CTAB) were bought from Alfa Aesar Corporation. 4-Bromobenzaldehyde dimethyl acetal, 4-chlorobenzaldehyde dimethyl acetal, 4-propylbenzaldehyde dimethyl acetal and 4-methylbenzaldehyde dimethyl acetal were purchased from J&K Corporation. All chemicals were used as received without any further purification. Ultrapure water was generated using a Millipore Milli-Q system with a Milli-pak filter of pore size 0.22 μm, and was used for the preparation of all aqueous solutions.

2.2. Preparation of MgAl-LDO@Al-MS nanocomposite

The hexagonal MgAl-LDH nanoplates were prepared by a previously reported method with some modifications, using coprecipitation followed by hydrothermal treatment.[33] In a typical synthesis, 40 mL of mixed metal salt aqueous solution containing 15 mmol of $MgCl_2 \cdot 6H_2O$ and 4 mmol of $AlCl_3 \cdot 6H_2O$ were coprecipitated with 160 mL NaOH solution (0.20 M) under vigorous stirring. The precipitates were gathered, dispersed in Na_2CO_3 solution (0.10 M) and stirred for 6 h. Then the precipitate was separated, washed with copious amounts of water, dispersed in pure deionized water and transferred to autoclaves. After hydrothermal treatment at 100 °C for 5 h, a homogeneous suspension was obtained. The MgAl-LDH nanoplates were collected by centrifugation for further use.

To coat the Al-containing mesoporous silica shell on the surface of the MgAl-LDH nanoplates, a surfactant-directed sol–gel process was used.[17,34,35] In brief, the MgAl-LDH nanoplates (200 mg) were first dispersed in a mixed solution containing deionized water (80 mL), ethanol (60 mL), CTAB (0.30 g) and 25 wt% $NH_3 \cdot H_2O$ (1140 μL). The mixture was subjected to ultrasonic treatment for 2 h, and then TEOS (300 μL) was added, followed by the addition of $Al(NO_3)_3 \cdot 9H_2O$ (130 mg). The as-obtained mixture was stirred for another 12 h. Finally, the solid was centrifuged from the reaction mixture, washed with deionized water and ethanol in turn, dried under vacuum and calcined at 475 °C, thus resulting in the MgAl-LDO@Al-MS nanocomposite.

2.3. Preparation of control samples

2.3.1. Preparation of MgAl-LDO nanoplates. MgAl-LDO nanoplates were obtained by the direct calcination of pure MgAl-LDH nanoplates at 475 °C for 5 h.

2.3.2. Preparation of Al-containing mesoporous silica (Al-MS). Al-MS was fabricated using the same preparation procedure as the MgAl-LDO@Al-MS composite without the addition of the MgAl-LDH nanoplates.

2.3.3. Preparation of pure mesoporous silica (MS). MS was prepared *via* the same synthesis route as the Al-containing mesoporous silica (Al-MS) without the addition of $Al(NO_3)_3 \cdot 9H_2O$.

2.4. One-pot deacetalization–Knoevenagel condensation reaction

Solid catalyst (40 mg) was added into a reaction mixture composed of toluene (3 mL), acetal (0.5 mmol), methyl cyanoacetate (1 mmol) and *para*-xylene (0.5 mmol) in a glass vessel. The resulting mixture was vigorously stirred at 110 °C for 2.0 h, and the reaction was stopped by cooling to room temperature. The solid catalyst was separated *via* centrifugation, and the filtrate was analyzed by gas chromatography (GC) (Agilent 6890N) with a capillary column (DB-5, 30.0 m × 320 μm × 0.25 μm) and flame ionization detection (FID), and the products were further confirmed by gas chromatography–mass spectrometry (GC-MS) (Shimadzu, GCMS-QP 2010S) with a capillary column (DB-5 ms, 30.0 m × 320 μm × 0.25 μm).

2.5. Characterization

The microscopic features of the samples were characterized using a scanning electron microscope (SEM, JEOL-6701F) equipped with an energy-dispersive X-ray (EDX) analyzer (Oxford INCA). Transmission electron microscopy (TEM) was carried out on a JEOL 2011F electron microscope running at 200 kV. EDX analysis was obtained with an EDAX system. Nitrogen adsorption–desorption isotherms were obtained on Quantachrome Autosorb AS-1 at 77 K. The wide-angle X-ray diffraction pattern was recorded on a Rigaku model D/MAX-2500V system (Cu Kα radiation) at 40 kV and 200 mA. Small-angle XRD measurements were carried out on a Rigaku D/max-2400 diffractometer equipped with a secondary graphite monochromator with Cu Kα radiation (wavelength $\lambda = 0.154$ nm). Data was collected in a step-scan mode in the range of 0.6–8° with step-width of 0.02° and speed of 1° min_{-1}. ^{27}Al solid-state NMR spectra were obtained on an AVANCE III 400 spectrometer operating at 104.1 MHz equipped with a 4 mm rotor spun at 5 kHz. The Mg and Al content in the material were analyzed using inductively coupled plasma atomic emission spectroscopy (ICP-AES, Shimadzu, ICPE-9000).

3. Results and discussion

The synthesis procedure for the multifunctional MgAl-LDO@Al-MS nanoplates is presented in Scheme 1a (see Experimental section for details). First, hexagonal MgAl-LDH nanoplates were prepared by coprecipitation followed by hydrothermal treatment. Then the hexagonal nanoplates were further coated with an Al-containing mesoporous silica shell *via* a surfactant-directed sol–gel strategy using TEOS as the silica precursor, $Al(NO_3)_3 \cdot 9H_2O$ as the alumina source and CTAB as a soft template. The MgAl-LDO@Al-MS nanocomposite was produced after calcination. For comparison, a series of control samples, *i.e.* MgAl-LDH, MgAl-LDO and Al-MS monofunctional catalysts, as well as pure MS were also fabricated (see Experimental section for synthesis details).

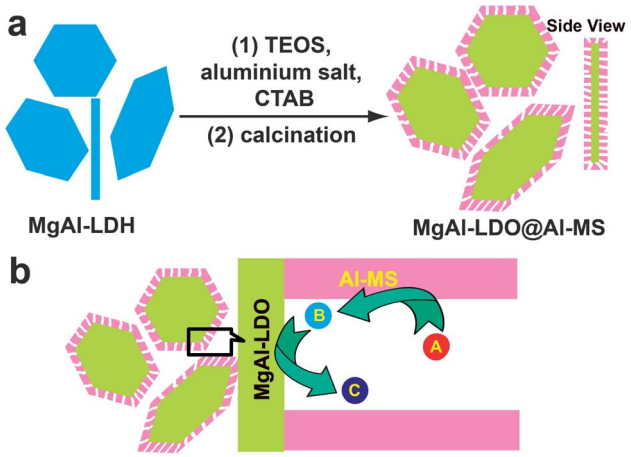

Scheme 1 (a) Synthesis procedure for acid–base bifunctional core–shell structured MgAl-LDO@Al-MS nanoreactors. (b) One-pot cascade reaction sequence conducted in the core–shell structured MgAl-LDO@Al-MS nanoreactor.

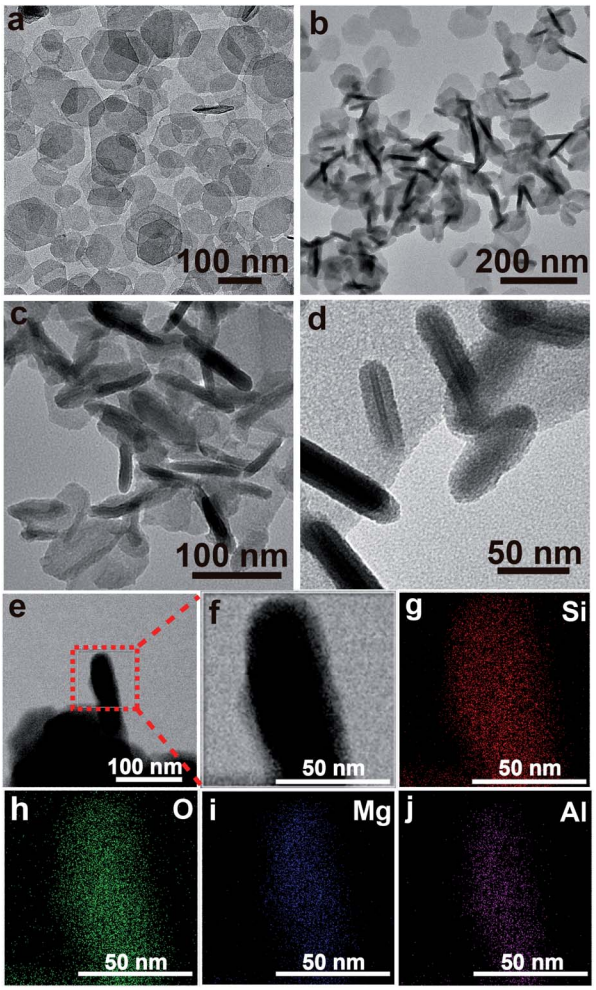

Fig. 1 (a) TEM image of the hexagonal MgAl-LDH nanoplates. (b–d) TEM images, (e and f) STEM images and (g) Si, (h) O, (i) Mg, (j) Al EDX elemental mappings of the MgAl-LDO@Al-MS nanocomposite.

The TEM image in Fig. 1a shows that the MgAl-LDH sample consists ofrelatively uniform hexagonal nanoplates with a lateral size in the range of 60–120 nm and a thickness of only 5–10 nm. The WAXRD patterns (Fig. 2a and b) indicate that MgAl-LDH has rhombohedral symmetry ($R\bar{3}m$) (JCPDF card no. 54-1030). After the hydrothermal treatment, the MgAl-LDH plates showed better crystallinity, with a (003) spacing of 0.78 nm. The atomic ratio of Mg : Al was 3.18, according to the ICP-AES analysis results.

Through the sol–gel shell coating and calcination process, the MgAl-LDO@Al-MS nanocomposite was obtained. From the TEM image (Fig. 1b), two kinds of nanostructures can be observed, which resulted from different projections of the as-obtained MgAl-LDO@Al-MS nanocomposite from two perpendicular directions. The SEM (Fig. S1 in SI†) and TEM images (Fig. 1c) show that the material retained its original hexagonal plate-like morphology and was uniform in size and shape, with a lateral size of 80–150 nm and a thickness of 25–35 nm. From the high magnification TEM image (Fig. 1d), the composite had a typical core–shell structure, the silica shell had a mesoporous structure with relatively disordered meso-channels, and the shell was well-covered on the MgAl-LDO inner core with a thickness of 10–15 nm. The STEM image (Fig. 1e), combined with the EDX elemental mappings (Fig. 1g–j), reveal that the elements Mg and Al existed in the inner core area, confirming that MgAl-LDO was covered by a mesoporous silica shell. Additionally, due to the low amount of Al content in the outer shell, the signal intensity of the outer shell Al was much weaker than that of Si and O, so the Al distribution in the outer shell was not obvious in the EDX elemental mapping.

The WAXRD pattern of MgAl-LDH@Al-MS (Fig. 2c) revealed that the LDH structure was maintained very well during the sol–gel shell coating process, and the broad diffraction peak at around 25° was assigned to the amorphous silica. The WAXRD

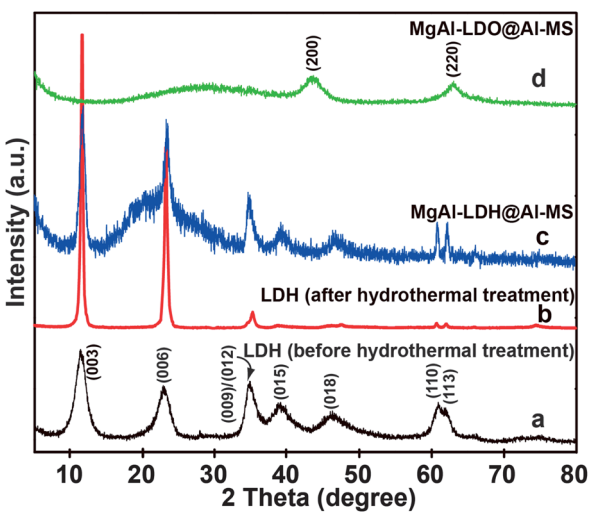

Fig. 2 Wide-angle XRD (WAXRD) patterns of (a) MgAl-LDH nanoplates before hydrothermal treatment, (b) MgAl-LDH nanoplates after hydrothermal treatment, (c) MgAl-LDH@Al-MS nanocomposite and (d) MgAl-LDO@Al-MS nanocomposite.

pattern of the corresponding calcination product MgAl-LDO@Al-MS exhibited the cubic phase MgO (JCPDF card no. 45-0946) (Fig. 2d). According to the previous report on hydrotalcite-derived mixed oxides,[20] the Al_2O_3 phase should also form, but in the amorphous phase, so it didn't show any peaks in the WAXRD pattern. ^{27}Al MAS NMR spectroscopic studies were performed to evaluate the Al^{3+} local atomic environment. The spectrum of the MgAl-LDO@Al-MS composite (Fig. S2†) displayed two main resonance signals at 67 and 9 ppm, which were assigned to tetrahedral (AlO_4), and octahedral (AlO_6) coordination, respectively.[36–38] EDX analysis of the MgAl-LDO@Al-MS composite further confirmed the presence of the elements Mg, Al Si and O (Fig. S3†), and ICP-AES analysis confirmed that the amounts of Mg and Al were 23.8 wt% and 11.2 wt%, respectively.

The nitrogen sorption analysis of samples MgAl-LDH showed a BET surface area, total pore volume, and average pore size of 45.7 $m^2\ g^{-1}$, 0.21 $cm^3\ g^{-1}$, and 12.2 nm, respectively (Fig. S4†). After shell coating and calcination, MgAl-LDO@Al-MS showed a large BET surface area (429 $m^2\ g^{-1}$), a high pore volume (0.41 $cm^3\ g^{-1}$) and a rather narrow pore size distribution centered at 2.7 nm (Fig. 3a). Moreover, the small-angle XRD pattern (Fig. 3b) of MgAl-LDO@Al-MS showed a broad diffraction peak indexed to the (100) reflection, further revealing the formation of somewhat disordered mesopores in the Al-containing silica outer shell.

In addition, characterizations (TEM, nitrogen adsorption–desorption measurement and SAXRD) were also performed on the control samples, MgAl-LDO and Al-MS monofunctional catalysts (detailed characterization information is listed in Fig. S5–S9 and Table S1†).

MgAl-LDO nanoplates, due to the surface O^{2-} species as well as trace OH^- resulting from adsorbed water on the surface, can act as a heterogeneous base,[39] while the mesoporous aluminosilicate shell can serve as a solid acid.[40] Thus, the MgAl-LDO@Al-MS nanoplates, in which the acid sites and basic sites were spatially separated through the core–shell structure design, could be used in acid–base bifunctional catalysis. Additionally, with basic sites on the surface of the inner core and acidic sites in the mesochannels of the mesoporous aluminosilicate shell, the MgAl-LDO@Al-MS nanocomposite may exhibit catalytic nanoreactor features during catalysis, *i.e.* the confined effect as well as the enrichment effect associated with the mesopores in the nanoreactor would be beneficial for fast catalytic reactions (Scheme 1b).

The catalytic performance of MgAl-LDO@Al-MS as an acid–base bifunctional heterogeneous catalyst was investigated in the one-pot acetal hydrolysis–Knoevenagel cascade reaction sequence. First, the catalytic activity of MgAl-LDO@Al-MS was compared with that of a series of control samples in the reaction between benzaldehyde dimethyl acetal and methyl cyanoacetate (reaction 1). As shown in Table 1, the MgAl-LDO@Al-MS nanocomposite was able to convert the acetal to the desired product in high yield (Table 1, entry 1), showing decent activity and selectivity. In contrast, a physical mixture composed of MgAl-LDO and Al-MS with similar concentration of catalytic sites was significantly less effective (Table 1, entry 9), demonstrating the advantage of the integration of both the acid and basic sites in one nanoreactor system with mesoporous channels and a core–shell structure. Additionally, the monofunctional catalysts MgAl-LDH and MgAl-LDO were inactive and could not produce desired target product, due to the lack of suitable acid sites (Table 1, entries 2 and 3). Monofunctional Al-MS has acid sites, so it could catalyze the acetal hydrolysis to some extent (Table 1, entry 4).

Interestingly, none of substrate **1** was converted to the product **3** when either homogeneous acid or base was added to the MgAl-LDO@Al-MS nanocomposite (Table 1, entries 5 and 6), because these homogeneous species can destroy the base or acid active sites on the solid catalyst. Pure

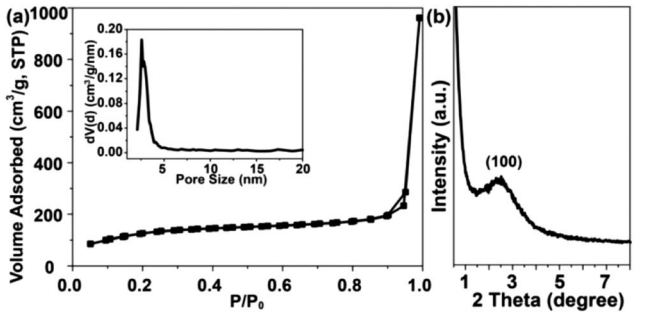

Fig. 3 (a) N_2 adsorption–desorption isotherm of the MgAl-LDO@Al-MS nanocomposite. Inset shows the NLDFT pore size distribution curve obtained from the desorption data. (b) Small-angle XRD pattern of the MgAl-LDO@Al-MS nanocomposite.

Table 1 One-pot acetal hydrolysis–Knoevenagel cascade reaction sequence catalyzed by various catalysts[a]

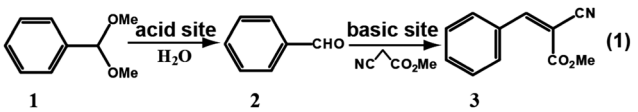

1 2 3

Entry	Catalyst	Conv. of **1** (%)	Yield of **2** (%)	Yield of **3** (%)
1	MgAl-LDO@Al-MS	100	3.6	96.4
2	MgAl-LDO	0	0	0
3	MgAl-LDH	0	0	0
4[b]	Al-MS	47.0	47.0	0
5	MgAl-LDO@Al-MS/AP	0	0	0
6	MgAl-LDO@Al-MS/PTSA	29.2	29.2	0
7	AP/PTSA	0	0	0
8	MS	0	0	0
9[c]	Physical mixture	90.0	33.0	57.0

[a] *Reaction conditions*: benzaldehyde dimethyl acetal (0.5 mmol), methyl cyanoacetate (1.0 mmol), toluene (3 mL), catalyst (40 mg), reaction temperature = 110 °C, reaction time = 2 h. Conversions and yields were determined using GC data. AP: 1-aminopropane, PTSA: *p*-toluene sulfonic acid. [b] Al-MS (12.7 mg; Al: 8.92 wt%). [c] Physical mixture composed of MgAl-LDO (27.3 mg; Mg: 34.9 wt%; Al: 12.3 wt%) and Al-MS (12.7 mg; Al: 8.92 wt%).

mesoporous silica (MS) didn't show any catalytic activity for the cascade reaction (Table 1, entry 8). The above results demonstrate that the formation of product **3** was catalyzed by solid acid for the deacetalization reaction, followed by the LDO solid base-catalyzed condensation reaction of methyl cyanoacetate with benzaldehyde. Note that the addition of water was not needed, probably owing to the presence of trace water in the reaction system under atmospheric conditions and/or the successive production of water in the second step of the cascade reaction sequence (the Knoevenagel reaction).[4]

The versatility of the MgAl-LDO@Al-MS bifunctional nanoreactor was also evaluated. MgAl-LDO@Al-MS was applied to reactions of several aromatic acetals with active methylene compounds (Table 2). The reaction of aromatic acetals with electron-withdrawing substituents with nitrile compounds proceeded smoothly and gave excellent yields of the corresponding products (Table 2, entries 2 and 3). In the case of aromatic acetals with electron-donating substituents, the yields were slightly diminished (Table 2, entries 4–6).

The recyclability of the MgAl-LDO@Al-MS nanocomposite was investigated using the one-pot cascade reaction between benzaldehyde dimethyl acetal and methyl cyanoacetate. The catalyst was recovered by centrifugation, washed with water, calcined at high temperature, and then reused in the next run. The results showed that the MgAl-LDO@Al-MS catalyst was robust and can be reused up to 4 times without significant loss of activity (Fig. 4a), demonstrating the high stability of our catalyst. From the TEM image in Fig. 4b, the catalyst that had been used repeatedly 4 times maintained the original morphology very well, suggesting that the mesoporous silica coating may help to maintain the mechanical integrity of the plate. The slight loss of catalytic reactivity of the MgAl-LDO@Al-MS nanocomposite in the recycling test may be attributed to the loss of some of the base or acid active sites during the reaction.

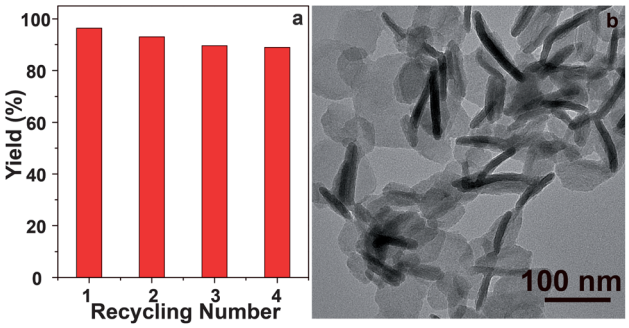

Fig. 4 (a) Recycling test of the MgAl-LDO@Al-MS nanocomposite in the reaction between benzaldehyde dimethyl acetal and methyl cyanoacetate. (b) TEM image of MgAl-LDO@Al-MS nanocomposite after being used as a bifunctional catalyst repetitively for 4 reactions.

The activity and selectivity of MgAl-LDO@Al-MS were relatively low compared to that of our previously reported acid–base bifunctional mesoporous silica nanospheres (MS-A@MS-B).[17] On MgAl-LDO@Al-MS, the base site activity is relatively low, as MgAl-LDO is a weak Lewis base, while the acidity of the Al-MS shell was sufficient. As shown in Table 2, the conversions of the first reaction, which is catalyzed by the acid sites, were 100% for all reactions, but the second reaction catalyzed by the base sites showed lower conversion. Thus, using a better catalyst with stronger base sites in the core part is a rational approach to improve the performance of the catalyst. Adding another basic component to the MgAl-LDO part of the composite is currently underway.

Table 2 MgAl-LDO@Al-MS-catalyzed one-pot acetal hydrolysis–Knoevenagel cascade reactions with different substrates[a]

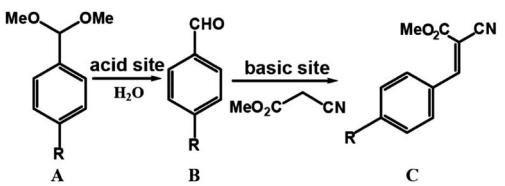

Entry	R	Conv. of **A** (%)	Yield of **B** (%)	Yield of **C** (%)
1	H	100	3.6	96.4
2	Cl	100	4.0	96.0
3	Br	100	5.0	95.0
4	CH_3	100	8.5	91.5
5	OCH_3	100	11.8	88.2
6	n-C_3H_7	100	14.6	85.4

[a] *Reaction conditions*: acetal (0.5 mmol), methyl cyanoacetate (1.0 mmol), toluene (3 mL), MgAl-LDO@Al-MS (40 mg), reaction temperature = 110 °C, reaction time = 2 h. Conversions and yields were determined using GC data.

4. Conclusions

In summary, we produced a core–shell structured MgAl-LDO@Al-MS inorganic nanocomposite with hexagonal Mg–Al mixed oxide nanoplates as the inner core and Al-containing mesoporous silica as the outer shell by a low cost route. The mesoporous silica shell was not only capable of protecting the MgAl-LDO core, but also offered a high surface area for the derivation of functional acid catalytic sites. Meanwhile, due to the good site-separation of the acid and basic sites *via* the core–shell structure design, the enrichment effect and the confined catalytic microenvironment provided by the nanoreactor system, the MgAl-LDO@Al-MS nanocomposite was an excellent acid–base bifunctional nanoreactor for one-pot deprotection–Knoevenagel cascade reaction sequences with high activity and selectivity.

Acknowledgements

We are grateful for the financial support from the National Basic Research Program of China (2009CB930400), the National Natural Science Foundation of China (NSFC 21273244, 21121063), and the Chinese Academy of Sciences (KJCX2-YW-N41).

Notes and references

1 F.-X. Felpin and E. Fouquet, *ChemSusChem*, 2008, **1**, 718.
2 M. J. Climent, A. Corma and S. Iborra, *Chem. Rev.*, 2011, **111**, 1072.
3 F.-X. Zhu, W. Wang and H.-X. Li, *J. Am. Chem. Soc.*, 2011, **133**, 11632.
4 S. Shylesh, A. Wagner, A. Seifert, S. Ernst and W. R. Thiel, *Chem.–Eur. J.*, 2009, **15**, 7052.
5 A. El Kadib, K. Molvinger, M. Bousmina and D. Brunel, *J. Catal.*, 2010, **273**, 147.
6 S. Shylesh and W. R. Thiel, *ChemCatChem*, 2011, **3**, 278.
7 K. Motokura, N. Fujita, K. Mori, T. Mizugaki, K. Ebitani and K. Kaneda, *J. Am. Chem. Soc.*, 2005, **127**, 9674.
8 E. Merino, E. Verde-Sesto, E. M. Maya, M. Iglesias, F. Sánchez and A. Corma, *Chem. Mater.*, 2013, **25**, 981.
9 J. Shi, *Chem. Rev.*, 2013, **113**, 2139.
10 F. Gelman, J. Blum and D. Avnir, *Angew. Chem., Int. Ed.*, 2001, **40**, 3647.
11 B. Helms, S. J. Guillaudeu, Y. Xie, M. McMurdo, C. J. Hawker and J. M. J. Frechet, *Angew. Chem., Int. Ed.*, 2005, **44**, 6384.
12 N. T. S. Phan, C. S. Gill, J. V. Nguyen, Z. J. Zhang and C. W. Jones, *Angew. Chem., Int. Ed.*, 2006, **45**, 2209.
13 N. R. Shiju, A. H. Alberts, S. Khalid, D. R. Brown and G. Rothenberg, *Angew. Chem., Int. Ed.*, 2011, **50**, 9615.
14 N. A. Brunelli, K. Venkatasubbaiah and C. W. Jones, *Chem. Mater.*, 2012, **24**, 2433.
15 S. Shylesh, A. Wagener, A. Seifert, S. Ernst and W. R. Thiel, *Angew. Chem., Int. Ed.*, 2010, **49**, 184.
16 Y. Huang, S. Xu and V. S. Y. Lin, *Angew. Chem., Int. Ed.*, 2011, **50**, 661.
17 L. Wang, J. Li, Q. Jiang and L. Zhao, *Dalton Trans.*, 2012, **41**, 4544.
18 J. Liu, H. Q. Yang, F. Kleitz, Z. G. Chen, T. Yang, E. Strounina, G. Q. Lu and S. Z. Qiao, *Adv. Funct. Mater.*, 2012, **22**, 591.
19 B. Wang, H. Wu, L. Yu, R. Xu, T.-T. Lim and X. W. Lou, *Adv. Mater.*, 2012, **24**, 1111.
20 P. Gunawan and R. Xu, *Chem. Mater.*, 2009, **21**, 781.
21 Y. Xu, Y. Dai, J. Zhou, Z. P. Xu, G. Qian and G. Q. M. Lu, *J. Mater. Chem.*, 2010, **20**, 4684.
22 Z. Zhang, Y. Zhang, Z. Wang and X. Gao, *J. Catal.*, 2010, **271**, 12.
23 H. Bao, J. Yang, Y. Huang, Z. P. Xu, N. Hao, Z. Wu, G. Q. Lu and D. Zhao, *Nanoscale*, 2011, **3**, 4069.
24 J. L. Gunjakar, T. W. Kim, H. N. Kim, I. Y. Kim and S.-J. Hwang, *J. Am. Chem. Soc.*, 2011, **133**, 14998.
25 M. Shao, F. Ning, J. Zhao, M. Wei, D. G. Evans and X. Duan, *J. Am. Chem. Soc.*, 2012, **134**, 1071.
26 C. u. G. Silva, Y. s. Bouizi, V. Fornés and H. García, *J. Am. Chem. Soc.*, 2009, **131**, 13833.
27 J. Liu, R. Harrison, J. Z. Zhou, T. T. Liu, C. Yu, G. Q. Lu, S. Z. Qiao and Z. P. Xu, *J. Mater. Chem.*, 2011, **21**, 10641.
28 S. Abelló, F. Medina, D. Tichit, J. Pérez-Ramírez, J. C. Groen, J. E. Sueiras, P. Salagre and Y. Cesteros, *Chem.–Eur. J.*, 2005, **11**, 728.
29 K. Ebitani, K. Motokura, K. Mori, T. Mizugaki and K. Kaneda, *J. Org. Chem.*, 2006, **71**, 5440.
30 M. Yang, J. Liu, Z. Chang, G. R. Williams, D. O'Hare, X. Zheng, X. Sun and X. Duan, *J. Mater. Chem.*, 2011, **21**, 14741.
31 S. Nishimura, A. Takagaki and K. Ebitani, *Green Chem.*, 2013, **15**, 2026.
32 F. Zhang, X. Zhao, C. Feng, B. Li, T. Chen, W. Lu, X. Lei and S. Xu, *ACS Catal.*, 2011, **1**, 232.
33 Z. P. Xu, G. S. Stevenson, C.-Q. Lu, G. Q. Lu, P. F. Bartlett and P. P. Gray, *J. Am. Chem. Soc.*, 2006, **128**, 36.
34 S.-W. Bian, Z. Ma, L.-S. Zhang, F. Niu and W.-G. Song, *Chem. Commun.*, 2009, 1261.
35 Z. Chen, Z.-M. Cui, F. Niu, L. Jiang and W.-G. Song, *Chem. Commun.*, 2010, **46**, 6524.
36 C. Boissière, L. Nicole, C. Gervais, F. Babonneau, M. Antonietti, H. Amenitsch, C. Sanchez and D. Grosso, *Chem. Mater.*, 2006, **18**, 5238.
37 Q. Yuan, A.-X. Yin, C. Luo, L.-D. Sun, Y.-W. Zhang, W.-T. Duan, H.-C. Liu and C.-H. Yan, *J. Am. Chem. Soc.*, 2008, **130**, 3465.
38 J. S. Valente, E. Lima, J. A. Toledo-Antonio, M. A. Cortes-Jacome, L. Lartundo-Rojas, R. Montiel and J. Prince, *J. Phys. Chem. C*, 2010, **114**, 2089.
39 F. Prinetto, G. Ghiotti, R. Durand and D. Tichit, *J. Phys. Chem. B*, 2000, **104**, 11117.
40 X. F. Qian, B. Li, Y. Y. Hu, G. X. Niu, D. Y. H. Zhang, R. C. Che, Y. Tang, D. S. Su, A. M. Asiri and D. Y. Zhao, *Chem.–Eur. J.*, 2012, **18**, 931.